URN (Paper): urn:nbn:de:gbv:ilm1-2011iwk-074:4

56TH INTERNATIONAL SCIENTIFIC COLLOQUIUM
Ilmenau University of Technology, 12 – 16 September 2011
URN: urn:nbn:gbv:ilm1-2011iwk:5

INVESTIGATIONS ON CLEARANCE SEAL UNITS FOR MOVING ELEMENTS IN AN ULTRA-HIGH VACUUM REGION

Nils Heidler[1,2], Matthias Mohaupt[1], Stefan Risse[1], Hans-Joachim Döring[3]

[1]Fraunhofer Institute for Applied Optics and Precision Engineering IOF, Jena, Germany;
[2]Institute of Applied Physics, Friedrich-Schiller-University, Jena, Germany
[3]Vistec Electron Beam GmbH, Jena, Germany

ABSTRACT

The steady demand of the semiconductor industry to achieve critical dimensions (cd) of 22 nm half pitch and below requires improved lithographic systems. Known approaches are the optical lithography in the short wavelength range (e.g. EUVL – Extreme Ultraviolet Lithography) or maskless lithography (e.g. EBL – Electron Beam Lithography). Both require a vacuum environment and a high positioning accuracy and stability of the mechanical elements. The positioning and guiding errors of wafer and mask stages or beam forming elements should therefore be at least one order of magnitude below the cd.

Within this paper, an EBL based application is described, that requires a high-precision movement within a high-vacuum environment. Different approaches for the mechanical feedthrough are reviewed which are enabled through the usage of a clearance seal unit. The chosen design options are examined by an experimental setup that is used to confirm the analytical evaluation.

Index Terms **–** ultra-high vacuum, E-beam, MSB, nanometer movement, contact-free seal unit

1. INTRODUCTION

The EBL is used for mask manufacturing as well as direct writing because of its capability to realize smaller structures than actual optical lithography systems. One way to enhance the comparably low throughput of E-beam systems is the multi-shaped beam (MSB) approach [1] [2] which is the further development of the single variable shaped beam (VSB).

The schematic realization of that concept is shown in *Figure 1*, depicting the deflection of a single beam and multiple beams into one direction.

It is based on the generation of parallel beamlets with the help of multi aperture diaphragm arrays (MAD). Every generated beamlet can be deflected into two directions with an electrostatic deflector array, the so-called Multi Beam Deflector (MBD).

Figure 2 shows the simplified setup of the mentioned elements within an electron optical column. It is necessary to use more than one array each to control the shape size, the beam on time and the position on target.

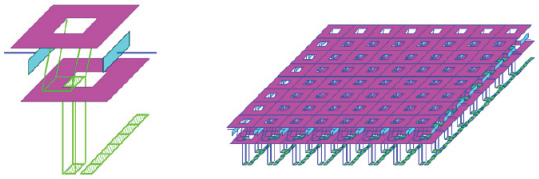

Figure 1: Schematic comparison of single Variable Shaped Beam VSB (left) and Multi Shaped Beam MSB (right) technique [2]

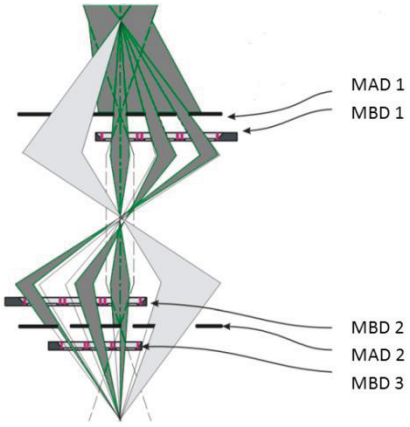

Figure 2: Simplified electron optical scheme of a column showing the combination of VSB path (light grey) and MSB path (dark grey)[2]

Thus it is necessary to adjust the position of every single MBD with respect to the optical axis as well as to the other MBD and MAD elements within a positioning accuracy below 200 nm. After reaching the position, the MBD has to hold a stable position of < 10 nm over a time frame of 10 minutes. An additional requirement is the positioning of the MBD in a high vacuum (HV) to ultra-high vacuum (UHV) environment $(< 10^{-5}\,Pa \text{ to } 10^{-6}\,Pa)$ that is mandatory to minimize the dispersion of the E-beam.
When considering the above mentioned requirements, it is obvious that the components (actuators, guides and measuring devices) and the whole system design have to be adequately chosen to meet the positioning

and stability accuracy as well as the vacuum specification. Two possible design options will be presented in the following chapters.

2. DESIGN OPTIONS

The components for moving and controlling the position of the MBD and the connections to the electrostatic deflectors of the MBD have a degassing rate, which can not be neglected in the intended vacuum range. Furthermore, the limited bake-out temperature of most of the components is disadvantageous. Therefore the MBD shall be spatial separated from these components while keeping the necessarily high positioning performance. This kind of flexible connection can be realized using a contact-free seal unit comprising evacuation grooves and successional seal gaps [3],[4] that enables a friction and stick-slip free feedthrough of the movement to the MBD. The seal gap generates an area of high flow resistance between to regions of different pressure, reducing the mass flow into the direction of the lower pressure. The evacuation groove is connected to a vacuum pump, discharging the major part of the gas coming through the previous seal gap.

The first design option for realizing the movement of the MBD within a UHV region is schematically shown in Figure 3.

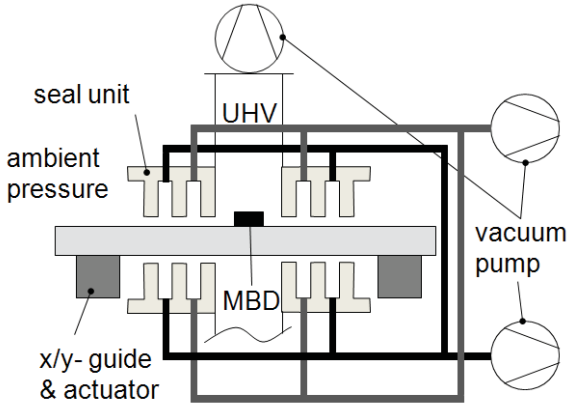

Figure 3: Schematic sectional view of design option 1 with MBD in UHV region and other components on ambient pressure

The rotational-symmetric seal unit comprises multiple seal gaps and according exhaustion grooves which surround the MBD and separates the UHV-region from the ambient pressure. This setup has the advantage, that no vacuum compatible elements for guiding, measuring and driving can be used. The necessary number of seal gaps and exhaustion grooves are disadvantageous since they increase the required space for the seal unit. Additionally, each stage needs its own vacuum pump what generates a higher technical and financial investment.

The design option 2 is schematically shown in Figure 4. That second design uses a simplified, rotational-symmetric seal unit with a single seal gap. This gap separates the outer vacuum region from the inner region with a higher vacuum. Both regions have to be evacuated by their own vacuum pump. Hence, the MBD is still placed inside a UHV region while all other components have to be chosen and designed to meet the medium vacuum to HV region requirements.

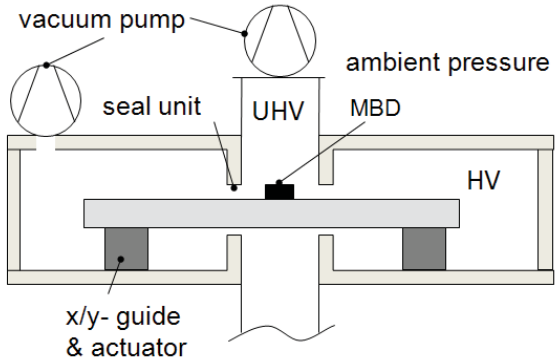

Figure 4: Schematic sectional view of design option 2 with MBD in UHV region and other components in HV region

3. ANALYTICAL EVALUATION

The main goal of the analytical calculation is to determine the feasibility of the seal unit of both design options. One consideration is the necessary geometrical dimension of the seal unit. The pressure in the UHV region as a target parameter has to be met.

3.1. Fundamentals

The calculation of the flow through the contact free seal unit is based on existing analytical formulas, considering the different kind of flows within the gap. The common classification into the molecular, the intermediate and the viscous flow is based on the Knudsen number Kn that is the ratio of the mean free path of the gas λ and the characteristic length of the element l_c , e.g. the height of the seal gap.

$$Kn = \frac{\lambda}{l_c} \tag{1}$$

Considering typical heights of seal gaps and the possible pressure range from ambient pressure (10^5 Pa) to UHV (10^{-5} Pa), the diagram in Figure 5 shows the transmission between the different kinds of flows based on the Knudsen number. It can be seen that all kind of flow can occur but the predominant one is the molecular flow. A widely used approach to simplify these considerations is to combine the analytical calculation of viscous and intermediate flow. This simplification leads during the calculations to a lower analytical pressure within the UHV region [5]. However, since the range of intermediate flow occurs only within a limited area of the seal gap and the majority of the flow regime is viscous or

molecular, this simplification does not serious limit the analytical accuracy.

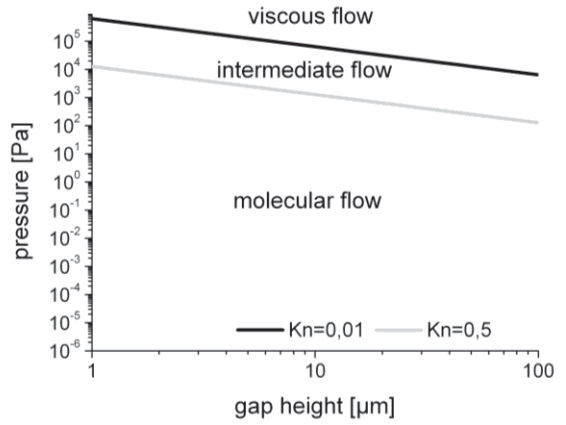

Figure 5: Transmission between flow regimes as a function of pressure and gap height

Based on the radial gap geometry of the two design options, the nomenclature given in Figure 6 will be used. Here, h denotes the gap height, r_i and r_o the radii of the inner and outer seal gap and p_i and p_o the pressure at the inner and outer boundary of the seal gap respectively.

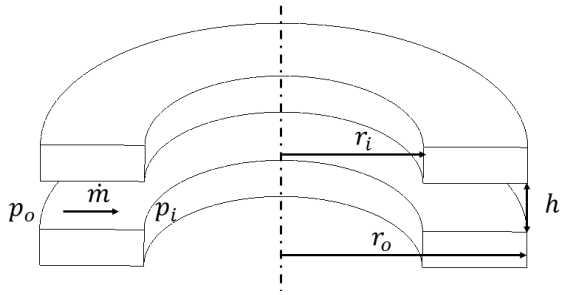

Figure 6: Declaration of parameters of a basic seal gap

Using the viscosity μ of the gas, the specific gas constant R_s and the temperature T, the mass flow rate $\dot{m}_{viscous}$ through a circular gap in the viscous range can be calculated [5].

$$\dot{m}_{viscous} = \frac{\pi h^3}{12\mu \ln\left(\frac{r_i}{r_o}\right) R_s T}\left(p_o^2 - p_i^2\right) \tag{2}$$

The mass flow rate $\dot{m}_{molecular}$ through the gap in the molecular range [5], [6] can be expressed by the following equation:

$$\dot{m}_{molecular} = \frac{\pi\,(r_0 + r_i)\,h^2\,\bar{c}}{4\,R_s T}\,\frac{ln\left[\frac{2(r_0 - r_i)}{h}\right] - \frac{1}{2}}{r_0 - r_i}(p_o - p_i) \tag{3}$$

This formula is based on the flow through the rectangular gap with the width $\pi\,(r_0 + r_i)$ and using the average molecular velocity $\bar{c} = \sqrt{\frac{8}{\pi} R_s T}$.

3.2. Calculation

With the mass flow rate $\dot{m}$ through the seal gap and the effective pumping speed S_{eff} within the exhaustion groove, the resulting pressure can be calculated:

$$p = \frac{\dot{m}\,R_S T}{S_{eff}} \tag{4}$$

The effective pumping speed within the exhaustion grooves can be calculated from the pumping speed of the vacuum pump S and the conductance C of the tubes between both.

$$^1/_{S_{eff}} = {}^1/_S + {}^1/_C \tag{5}$$

Since these parameters depend on the used vacuum pump and the setup itself, the analytical derivation of the effective pumping speed and the conductance will not be discussed in detail. For more information on the calculation of the conductance over different flow regimes, see e.g. [6],[7].

For a comparable survey of the analytical results, some parameters are kept constant while the changes of the others are determined, see Table 1. They were chosen to fit to the later experimental investigations.

The effective pumping speed for the calculation is set to 0,08 m³/s. This can be realized by using different kind of vacuum pumps for different pressures and by keeping the conductance of the tubes high.

Table 1: Parameters

Parameter	Magnitude
r_i	20.0 mm
r_o	32.5 mm
S_{eff}	0.08 m^3/s
h	5 µm … 100µm
p_o	< 100.000 Pa

3.3. Results

The following results are based on room temperature ($T = 293\,K$) and the usage of nitrogen ($R_S = 296.8\,\frac{J}{kg\,K}$).

Using the equations (2) - (5) and the parameters in Table 1, p_i is plotted within Figure 7 against p_o for different gap heights. The high slope of the curves at higher pressures and for increasing gap heights in Figure 7 results from the transmission between the flow regimes. This diagram can help to determine the number of seal gaps and exhaustion grooves for different seal gap heights.

While using these calculations for the evaluation of the described design options, it must be considered, that they comprise two seal units (upper and lower one).

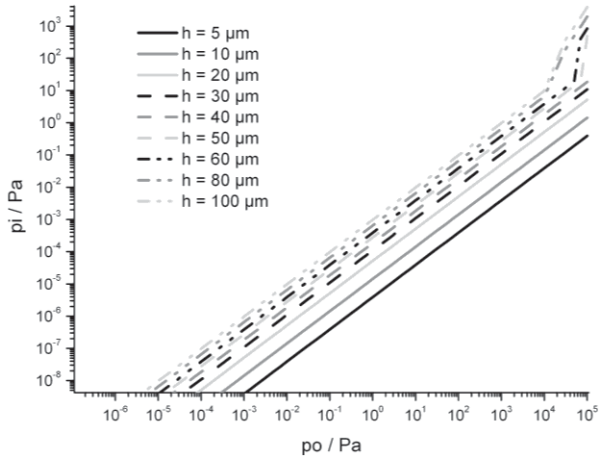

Figure 7: analytical obtained pressure p_i over p_o for different gap heights h

Regarding design option 1 and assuming a typical gap height of 50 µm, three exhaust grooves between the outer and inner area would be necessary to realize a pressure of $p_i < 10^{-5}$ Pa. Considering a length of the seal gap of approx. 10 mm in order to keep a high flow resistance and a length of the exhaust grooves of approx. 15 mm in order to realize a high conductance between the groove and the attached vacuum pump, the diameter of the seal unit would exceed 160 mm. That would necessitate the fabrication of surfaces with an accordingly low form deviation (e.g. one order of magnitude lower than the gap height) over a large area. The operational errors (straightness, roll, pitch) of the used guides should be in the same order of magnitude as the form deviation.

The pressure p_o of design option 2 has to be below 10^{-2} Pa. The above mentioned restrictions do apply here as well, but for a reduced diameter of approx. 65 mm.

4. EXPERIMENTAL SETUP

To verify the theoretical computation for the two design options, an experimental setup will be used. In order to achieve a setup with a reduced complexity and to enable the characterization of both options for a broad set of input parameters, a flexible setup was developed; see Figure 8 and Figure 9.

It uses one seal gap which is located between the upper and the lower part of the setup. The gap height can be adjusted with the help of three micrometer screws which are attached at the upper part. Three capacitive probes at the upper part can directly measure the gap height. The lower part is mounted to the vacuum chamber and the upper one is placed on top. Thereby, an inner and an outer area are created (compare Figure 6) which can be connected to separate vacuum pumps. The radii r_i and r_o of the seal gap is similar to those, used during the analytical calculations (see Table 1).

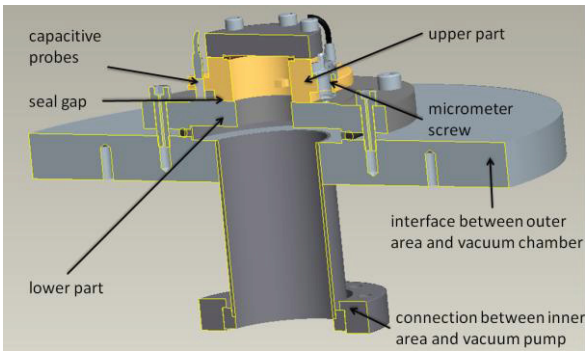

Figure 8: Sectional-view of experimental setup

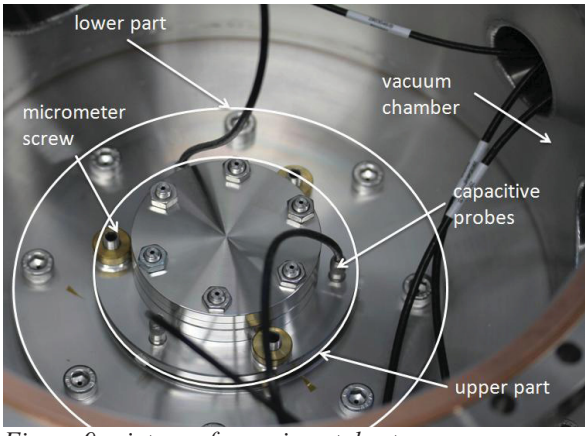

Figure 9: picture of experimental setup

The pressure in the outer area is measured by a Pirani gauge and the inner area by a combined Pirani and Bayard-Alpert ion gauge.

To realize the wide pressure range, different vacuum pumps have to be used. In the first setup, the outer area is at ambient pressure, while the inner area is evacuated by a rotary vane pump ($S = 0{,}01\ m^3/s$). In the second setup, the outer area is evacuated by the rotary vane pump and the inner area by a turbo molecular pump ($S = 0{,}08\ m^3/s$).

The usage of a precision inlet valve in the second setup allows for the adjustment of the pressure within the outer area. The measurement starts with the lowest reachable pressure (valve closed) and is than stepwise increased till the highest allowable pressure at the vacuum pump is reached. This procedure is reiterated with different gap heights.

The shape and the roughness of the sealing surfaces of the setup where characterized since they influence the effective gap height and hence the flow through the seal gap. They are fabricated by turning and have a root mean square (RMS) roughness of 0,2 µm to 0,7 µm and a form deviation of ± 4 µm.

The initial state for the experimental investigations is the direct contact of the two sealing surfaces. This position is set to a gap height of 16 µm, due to the form deviation of both surfaces.

5. RESULTS

The results for the pressure in the inner area of the first setup with $p_o = 100{,}000\,Pa$ and different gap heights are shown in Figure 10. It can be seen, that the measured results are slightly below the calculated results. It should be pointed out, that the uncertainty of measurement of vacuum gauges in the range between ambient pressure and $10{,}000\,Pa$ is around 100 % of the measured value. Below $10{,}000\,Pa$ it is still 10 %.

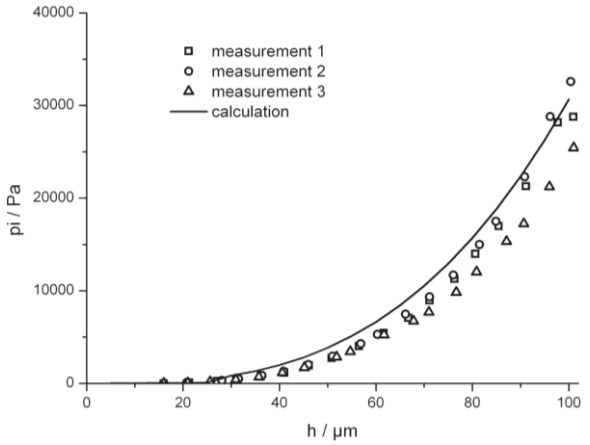

Figure 10: pressure in inner area over gap height (p_o = 100000 Pa)

The second setup is evaluated, using three gap heights ($h = 16\,\mu m, h = 24\,\mu m, h = 42\,\mu m$). The results can be seen in Figure 11 to Figure 13.

While the results between the measured and the calculated pressure for the gap height of $16\,\mu m$ differ by a factor of 2, the results for 24 µm and 42 µm are in a good agreement. It is assumed, that the gap is not uniform during the direct mechanical contact of the sealing surfaces. This could cause the deviation of the results in Figure 11.

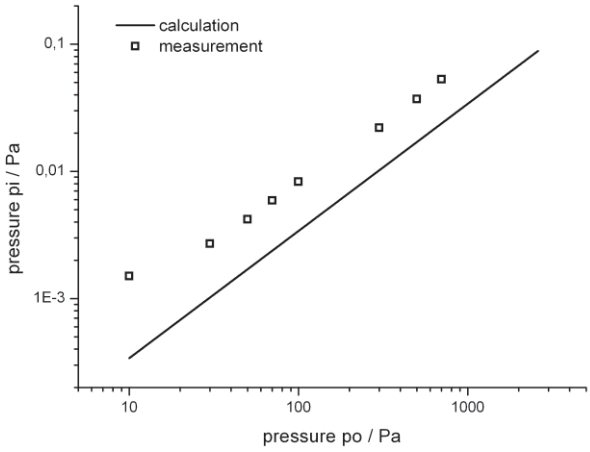

Figure 11: pressure in inner area over pressure in outer area (h = 16 µm)

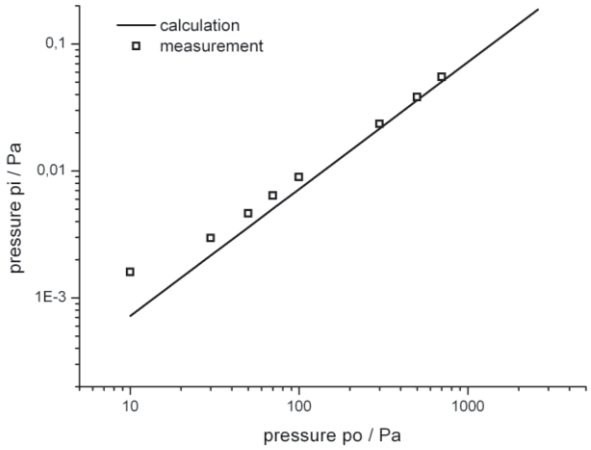

Figure 12: pressure in inner area over pressure in outer area (h = 24 µm)

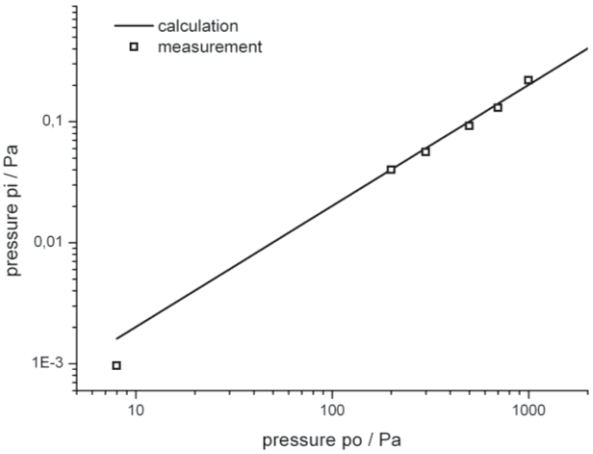

Figure 13: pressure in inner area over pressure in outer area (h = 42 µm)

The lowest measured pressure for a typical gap height of approximately 50 µm, which was achieved with the used experimental setup, was $p_i = 9.6 \cdot 10^{-4}\,Pa$ at $p_o = 8\,Pa$ with a gap height of $h = 42\,\mu m$ (see Figure 13). The inlet valve was exchanged by a blank flange for this measurement. The comparably high pressure in the outer area is most likely due to the used capacitive probes, vacuum gauges and the inlet valve. They are connected to the vacuum chamber using KF flanges with an elastomeric O-ring. By replacing all connections with CF flanges (copper gasket) it is presumable that a lower pressure in the outer and hence in the inner area is achievable.

6. CONCLUSION

Regarding the analytical results, both design options are in general feasible. The experimental results verify these calculations.

The main restriction for design option 1 is the number of necessary exhaustion grooves and the related number of evacuation tubes and vacuum pumps. Evacuation tubes with an appropriate high

conductance would require an accordingly large space within the vacuum chamber. This could lead to the minimization of the diameter of the tubes and hence to a lower effective pumping speed and a higher pressure within the inner area. Using more mechanical vacuum pumps could generate unwanted vibrations, which can be transmitted to the MBD. That could significantly influence the requirement of holding a stable position of < 10 nm over a time frame of 10 minutes. This would adversely affect the performance of the whole system.

The main restriction of the design option 2 is the required HV in the outer area. This demands a vacuum compatible design and leads to a limited choice for guides, actuators and probes. The main advantages are the simple design concerning vacuum generation, the simplified fabrication of the sealing system and the prevention of disturbing vibrations, which makes this the favorable option.

7. OUTLOOK

The presented setup shall be further used to investigate the conductance of the whole MBD system including the upper and lower seal unit and the aperture like design of the MBD itself. This is useful to estimate the pressure distribution within the UHV area along the beam path.

8. ACKNOWLEDGMENT

This work was supported by the Thüringer Aufbaubank with funds provided through EFRE (Europäische Fonds für regionale Entwicklung) under project PARCEL - Parallel shaped electron beam lithography - FK 2010FE9028.

9. REFERENCES

[1] US 7,741,620 B2, Multi-beam modulator for a particle beam and use of the multi-beam modulator for the maskless structuring of a substrate, Vistec, 2010

[2] M. Slodowski, H-J. Doering, W. Dorl and I. A. Stolberg, Multi-shaped beam proof of lithography, Proc. SPIE 7637, 2010, doi:10.1117/12.846529

[3] US 4,726,689, Linear gas bearing with integral vacuum seal for use in serial process ion implantation equipment, Eclipse Ion Technology Inc., 1988

[4] N. Heidler, C. Schenk, G. Harnisch, S. Risse, G. Schubert, R. Eberhardt, A. Tünnermann, “Dynamical non-contact exhaustion pipe for vacuum compatible air guided stages”, Proceedings 24th ASPE Meeting, 2009

[5] D. Trost, “Design and analysis of hydorstatic [sic] gas bearings for vacuum applications”, Proceedings 21st ASPE Meeting, 2006

[6] M.Wutz, Handbuch Vakuumtechnik, Friedr. Vieweg & Sohn Verlag, 2004

[7] P.Fan, „A stratified flow model for calculating the conductance of long tubes with constant cross section”, Vacuum 60, pp. 347-354, 2001